SRp55 Regulates a Splicing Network That Controls Human Pancreatic β-Cell Function and Survival

Jonàs Juan-Mateu,[1] Maria Inês Alvelos,[1] Jean-Valéry Turatsinze,[1] Olatz Villate,[1] Esther Lizarraga-Mollinedo,[1] Fabio Arturo Grieco,[1] Laura Marroquí,[1] Marco Bugliani,[2] Piero Marchetti,[2] and Décio L. Eizirik[1,3]

Diabetes 2018;67:423–436 | https://doi.org/10.2337/db17-0736

Progressive failure of insulin-producing β-cells is the central event leading to diabetes, but the signaling networks controlling β-cell fate remain poorly understood. Here we show that SRp55, a splicing factor regulated by the diabetes susceptibility gene *GLIS3*, has a major role in maintaining the function and survival of human β-cells. RNA sequencing analysis revealed that SRp55 regulates the splicing of genes involved in cell survival and death, insulin secretion, and c-Jun N-terminal kinase (JNK) signaling. In particular, SRp55-mediated splicing changes modulate the function of the proapoptotic proteins BIM and BAX, JNK signaling, and endoplasmic reticulum stress, explaining why SRp55 depletion triggers β-cell apoptosis. Furthermore, SRp55 depletion inhibits β-cell mitochondrial function, explaining the observed decrease in insulin release. These data unveil a novel layer of regulation of human β-cell function and survival, namely alternative splicing modulated by key splicing regulators such as SRp55, that may cross talk with candidate genes for diabetes.

Diabetes is caused by loss and/or functional impairment of insulin-producing pancreatic β-cells. Type 1 diabetes (T1D) and type 2 diabetes (T2D) differ in their genetic background, associated environmental factors, and clinical history, but both forms of diabetes show loss of β-cell mass, which is near total in long-term T1D and in the range of 20–50% in T2D (1–3). The mechanisms leading to this decrease in functional β-cell mass remain elusive, which may explain why intervention trials aiming to halt or revert β-cell loss in diabetes have consistently failed.

Genetic variations in the transcription factor *GLIS3* are associated with susceptibility to both T1D and T2D (4,5). *GLIS3* mutations also cause a neonatal diabetes syndrome characterized by neonatal diabetes, congenital hypothyroidism, and polycystic kidney (6). Functional studies have shown that *GLIS3* regulates β-cell differentiation and insulin transcription (7,8). We showed that *GLIS3* is also required for adult β-cell survival, increasing basal apoptosis when depleted in rodent and human β-cells and sensitizing these cells to cytokine- and palmitate-induced apoptosis (9). Increased β-cell apoptosis in *Glis3*-depleted β-cells in rats is associated with inhibition of the splicing factor SRp55 (also known as *Srsf6*), leading to a splicing shift in the proapoptotic protein Bim that favors the expression of the most prodeath splice variant Bim S (9).

Alternative splicing (AS) is a key posttranscriptional mechanism in which different combinations of splice sites in the precursor mRNA are selected to generate structurally and functionally distinct mRNA and protein variants. Functionally related transcript populations are regulated by master splicing factors in coordinated "splicing networks" that modulate cell-, tissue-, or developmental-specific functions (10,11). Little is known of the role of AS in diabetes, but recent findings by our group indicate that neuron-enriched splicing factors play important roles in β-cell function and survival (12,13) and that inflammatory and metabolic

[1]ULB Center for Diabetes Research, Medical Faculty, Université Libre de Bruxelles, Brussels, Belgium
[2]Department of Clinical and Experimental Medicine, Islet Cell Laboratory, University of Pisa, Pisa, Italy
[3]WELBIO, Université Libre de Bruxelles, Brussels, Belgium

Corresponding authors: Décio L. Eizirik, deizirik@ulb.ac.be, and Jonàs Juan-Mateu, mjuanmat@ulb.ac.be.

Received 30 June 2017 and accepted 6 December 2017.

This article contains Supplementary Data online at http://diabetes.diabetesjournals.org/lookup/suppl/doi:10.2337/db17-0736/-/DC1.

J.J.-M. and M.I.A. are joint first authors.

L.M. is currently affiliated with the Cellular Physiology and Nutrition Research Group, Bioengineering Institute, Miguel Hernández University, Elche, Spain.

stresses induce different "AS signatures" in human β-cells (14,15).

The splicing factor SRp55 has been implicated in wound healing and oncogenesis, acting as an oncoprotein that promotes cell proliferation, cell survival, and hyperplasia in cancer (16,17). In this study, we analyzed the global role of SRp55 in β-cell function and survival using human pancreatic islets and the human insulin-producing EndoC-βH1 cell line. We found that SRp55 deficiency leads to increased β-cell apoptosis, impaired mitochondrial respiration, and defective insulin secretion. These findings indicate that SRp55 is a key downstream mediator of *GLIS3* function, suggesting that splicing networks regulated by the cross talk between master splicing factors and candidate genes may contribute to β-cell dysfunction and death in diabetes.

RESEARCH DESIGN AND METHODS

Culture of Human Islets and EndoC-βH1 Cells

Human islets from donors without diabetes were isolated in Pisa, Italy, using collagenase digestion and density gradient purification. Islets were cultured at 6.1 mmol/L glucose as described previously (14). Donor characteristics are described in Supplementary Table 1. Human insulin-producing EndoC-βH1 cells were provided by Dr. R. Sharfmann (Institut Cochin, Université Paris Descartes, Paris, France); they were grown on plates coated with Matrigel and fibronectin (100 and 2 μg/mL, respectively) and cultured in DMEM as previously described (18). In some experiments EndoC-βH1 cells were exposed to the human cytokines interleukin-1β (50 units/mL; R&D Systems, Abingdon, U.K.) and interferon-γ (1,000 units/mL; Peprotech, London, U.K.) for 48 h, as described previously (14).

Gene/Splice Variant Silencing and Overexpression

The small interfering RNAs (siRNA) targeting the human genes/splice variants used in this study are described in Supplementary Table 2; Allstars Negative Control siRNA (Qiagen, Venlo, Netherlands) was used as a negative control (siCTL). Transient transfection was performed using 30 nmol/L siRNA and Lipofectamine RNAiMAX (Invitrogen, Carlsbad, CA). A pcDNA FLAG plasmid containing the human cDNA sequence of *SRSF6* (SRp55), provided by Professor Hirokazu Hara (Gifu Pharmaceutical University, Gifu, Japan), was used to exogenously express SRp55 in EndoC-βH1 cells.

Assessment of Cell Viability

Cell viability was determined using fluorescence microscopy after incubation with the DNA-binding dyes Hoechst 33342 and propidium iodide, as described previously (19). In some experiments apoptosis was further confirmed by immunostaining for cleaved caspase-3.

RNA Sequencing

Total RNA was isolated from five independent preparations of EndoC-βH1 cells exposed to control (siCTL) or SRp55 (siSR#2) siRNA using the RNeasy Mini Kit (Qiagen, Venlo, the Netherlands). RNA sequencing was performed on an Illumina HiSEq 2000 Sequencing System as previously described (12,20). The raw data generated were deposited in Gene Expression Omnibus under submission number GSE98485.

RNA Sequencing Analysis

RNA sequencing reads were mapped to the human reference genome GRCh37/hg19 using TopHat 2 (14) and the Gencode annotation data set. Transcript abundance and differential expression were calculated using Flux Capacitor (21). All genes and transcripts have been assigned a relative expression level as measured in reads per kilobase per million mapped reads (RPKM). A gene/isoform was considered to be expressed if it had a RPKM $\geq$0.5. Up- and downregulated genes were identified by computing the Fisher exact test and corrected by the Benjamini-Hochberg method, as previously described (14). A minimum of 17% change (log two-fold change of $\pm$0.23) in the expression level between SRp55 knockdown (KD) and control was considered to be "modified expression."

AS events were analyzed using rMATS (22), which computes percentage splicing index (PSI) and the false discovery rate (FDR) for five different splicing events: skipped exons, mutually exclusive exons, retained introns, and 5′ and 3′ alternative splice sites. To identify significant changes, we used the cutoffs of 5% on ΔPSI and of 0.01% on FDR. Motif enrichment was analyzed in the vicinity of alternatively spliced exons using rMAPS (23) by comparing the spatial occurrence of two SRp55 motifs (17,24) between cassette exons whose inclusion is affected by SRp55 KD and non-modified exons showing an FDR $\geq$50%.

Functional annotation and pathway enrichment of genes presenting splicing and/or gene expression alterations were analyzed using the Database for Annotation, Visualization and Integrated Discovery and Ingenuity Pathway Analysis platforms (25).

Validation of Splicing Changes by RT-PCR

Selected alternative splicing changes identified by RNA sequencing was validated by RT-PCR using exonic primers (Supplementary Table 3) encompassing the predicted splicing event. The primers were designed against flanking constitutive exons, allowing different splice variants to be distinguished based on fragment size. cDNA was amplified using MangoTaq DNA polymerase (Bioline), and PCR products were separated using the LabChip electrophoretic Agilent 2100 Bioanalyzer system and the DNA 1000 LabChip kit (Agilent Technologies, Wokingham, U.K.). The molarity of each PCR band corresponding to a specific splice variant was quantified using the 2100 Expert Software (Agilent Technologies, Diegem, Belgium), and used to calculate the ratio between inclusion and exclusion of the alternative event.

mRNA Extraction and Quantitative (Real-time) PCR

Poly(A)+ mRNA was isolated using the Dynabeads mRNA DIRECT Kit (Invitrogen, Carlsbad, CA) and reverse transcribed as described previously (19). Quantitative (real-time) PCR was performed using SYBR and concentrations

were calculated as copies per microliter using a standard curve (26). Gene expression was corrected for the reference gene β-actin. The primers used are listed in Supplementary Table 3.

Western Blotting and Immunofluorescence

For Western blotting, cells were washed with cold PBS and lysed in Laemmli buffer. Total proteins were resolved by 8–14% SDS-PAGE, transfected to a nitrocellulose membrane, and immunoblotted using the specific primary antibodies listed in Supplementary Table 4. Densitometric values were corrected with the housekeeping protein α-tubulin as the loading control, after background subtraction. Double immunostaining was performed as previously described (9).

Insulin Secretion

EndoC-βH1 cells were preincubated with culture medium containing 2.8 mmol/L glucose for 18 h. Cells were incubated in Krebs-Ringer buffer for 1 h and sequentially stimulated with 1 mmol/L glucose, 20 mmol/L glucose, or 20 mmol/L glucose and 10 μmol/L forskolin for 40 min, as described elsewhere (27). Insulin release and insulin content were measured in cell-free supernatants and acid/ethanol-extracted cell lysates, respectively, using a human insulin ELISA kit (Mercodia, Uppsala, Sweden). Results were normalized by total protein content.

Mitochondrial Respiration

Oxygen consumption rates of EndoC-βH1 cells were measured using the XFp Extracellular Flux Analyzer (Seahorse Bioscience, North Billerica, MA) as previously described (27). After transfection, cells were preincubated in assay medium containing 1 mmol/L glucose at 37°C in air for 1 h. After that, respiration was measured following sequential injections of 20 mmol/L glucose, 5 μmol/L oligomycin, 4 μmol/L carbonyl cyanide-p-trifluoromethoxy-phenylhydrazone (FCCP), and 1 μmol/L rotenone plus 1 μmol/L antimycin A. All data were normalized with total DNA content.

Statistical Analysis

Data are shown as mean ± SD. Significant differences between experimental conditions were assessed by a paired Student *t* test or by ANOVA followed by Bonferroni correction, as indicated. *P* values <0.05 were considered statistically significant.

RESULTS

SRp55 Regulates Human β-Cell Survival

Fluorescence microscopy indicated that SRp55 is highly expressed in pancreatic β-cells (Fig. 1*A*). SRp55 mRNA expression is higher in human pancreatic islets and human insulin-producing EndoC-βH1 cells than in eight other human tissues (Fig. 1*B*). To study the functional impact of SRp55 depletion on human β-cell survival, we silenced SRp55 using two specific siRNAs in human islets and EndoC-βH1 cells, reaching ≥50% inhibition at both the mRNA and protein levels (Fig. 1*C*, *E*, and *F*). SRp55 silencing significantly increased β-cell death in both dispersed human islets and in EndoC-βH1 cells (Fig. 1*D* and *G*). The observed increase in cleaved caspase-3 expression in SRp55-depleted cells confirms that β-cell loss is mediated by apoptosis (Fig. 1*H* and *I*). Next, we analyzed whether SRp55 expression is affected by proinflammatory cytokines. Exposure of EndoC-βH1 cells to interleukin-1β and interferon-γ significantly decreased SRp55 protein expression (Supplementary Fig. 1*A*). Overexpression of SRp55 in EndoC-βH1 cells (Supplementary Fig. 1*B*) protected these cells against cytokine-induced apoptosis (Supplementary Fig. 1*B*), suggesting that decreased SRp55 expression may contribute to β-cell death during islet inflammation.

Identification of SRp55-Regulated Splicing Events by RNA Sequencing

SRp55-regulated splicing events were detected by RNA sequencing of five independent EndoC-βH1 preparations under control conditions or after SRp55 KD, obtaining average coverage of 166 million reads. A total of 8,769 AS events were detected as modified after SRp55 KD (Fig. 2*A* and Supplementary Table 5). The majority of modified AS events correspond to cassette exons (59%), followed by mutually exclusive exons (22%), alternative 5′ splice site (9%), alternative 3′ splice site (7%), and intron retention (3%) (Fig. 2*B*).

Modified AS events affected 4,055 different genes (Supplementary Table 5). Functional enrichment analysis indicated that genes showing AS changes after SRp55 KD depletion are involved in diverse molecular and cellular functions, including cell cycle, DNA repair and replication, cell death and survival, and cellular function and maintenance (Fig. 2*C*). Enriched pathways included several pathways involved in pancreatic β-cell function, dysfunction, and death (Fig. 2*D*), including genes related to T2D and insulin secretion, regulation of apoptosis, and c-Jun N-terminal kinase (JNK) signaling (Fig. 2*D*).

SRp55 KD had a less marked impact on gene transcription when compared with RNA splicing (Supplementary Fig. 2*A* and *B*). Nevertheless, SRp55 KD modified the expression of 2,981 genes, inducing predominantly gene upregulation (Supplementary Fig. 2*C* and Supplementary Table 6). Of note, 28% of differentially expressed genes also presented changes on AS (Supplementary Fig. 2*D*). Upregulated genes were enriched in pathways involved in the cell cycle, DNA repair and replication, and mitogen-activated protein kinase signaling, among others (Supplementary Table 6).

SRp55 Binding Motif Analysis

To study whether alternatively spliced genes are directly regulated by SRp55 and to identify spatial patterns of SRp55 binding, we performed an enrichment analysis of the SRp55 binding motifs. We compared the occurrence of SRp55 motifs between modified cassette exons and exons unaffected by SRp55 silencing. We analyzed the enrichment of two SRp55 motifs: a 6-mer motif identified by SELEX (24), and a 9-mer motif identified by de novo discovery in modified exons after SRp55 overexpression in mouse skin (17) (Supplementary Fig. 3*A*). Significant enrichment for both motifs in exonic regions was found in downregulated

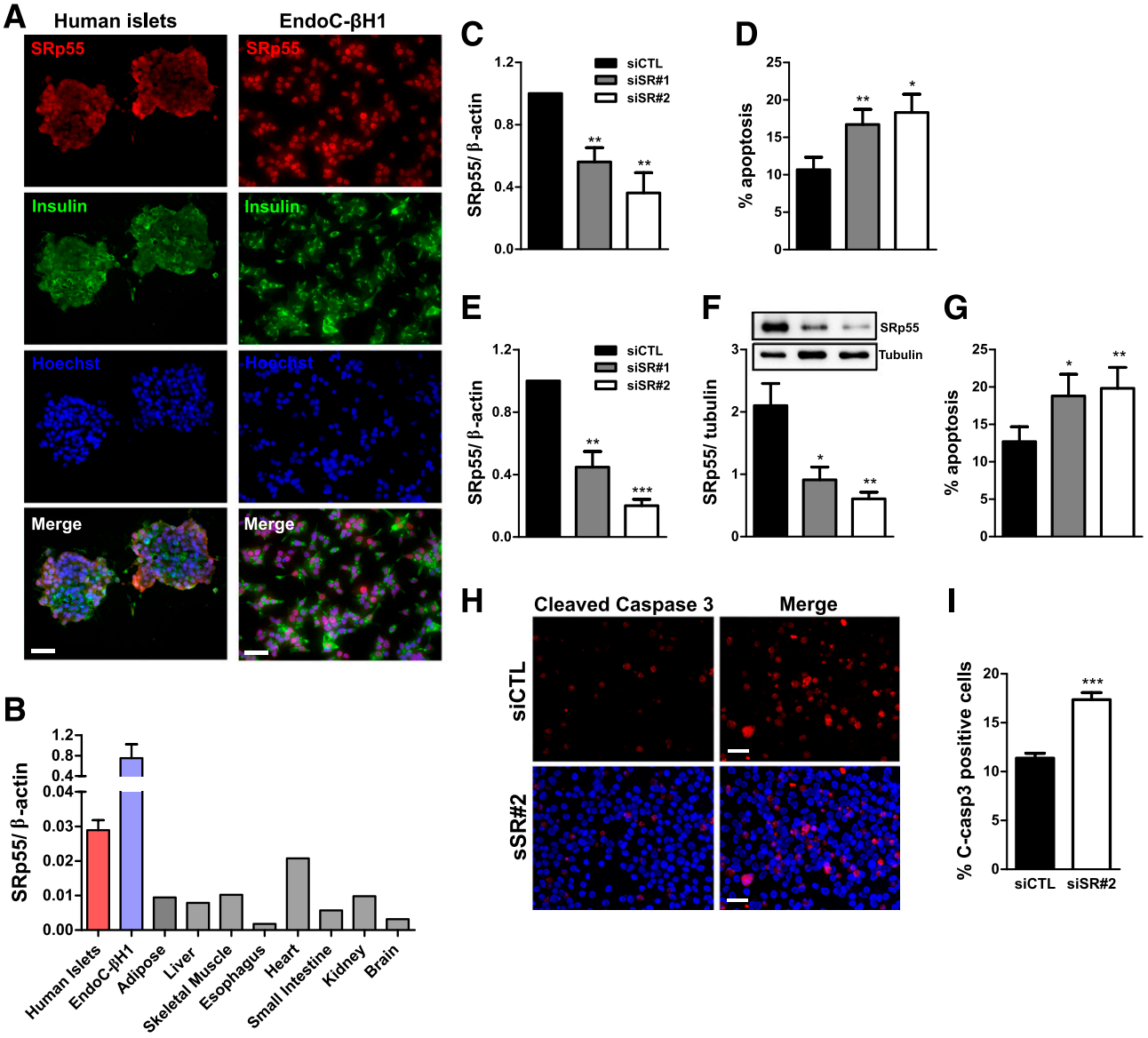

Figure 1—SRp55 is highly expressed in human pancreatic β-cells, and its depletion leads to increased β-cell apoptosis. *A*: Fluorescence microscopy of insulin and SRp55 in human islets (left panel) and in the human EndoC-βH1 cell line (right panel) shows staining of SRp55 (red), insulin (green), and nuclei (blue). *B*: mRNA expression of SRp55 in human islets, EndoC-βH1 cells, and a panel of normal human tissues was measured by quantitative RT-PCR (qRT-PCR) and normalized by the housekeeping gene β-actin. *C* and *D*: Human islets were transfected with siCTL or specific siRNA against SRp55 (siSR#1 and siSR#2) for 48 h. SRp55 KD levels were assessed by qRT-PCR (*C*), and apoptosis was evaluated by Hoechst/propidium iodide (PI) staining (*D*). *E–I*: EndoC-βH1 cells were transfected with control or specific siRNA against SRp55 for 48 h. SRp55 KD levels were assessed by qRT-PCR (*E*) and by Western blotting (*F*). Apoptosis of EndoC-βH1 cells after SRp55 KD was evaluated by Hoechst/PI staining (*G*) and by cleaved caspase 3 immunofluorescence (*H* and *I*). Scale bars = 1 μm. Results are the mean ± SEM of three to nine independent experiments. **P* < 0.05, ***P* < 0.01, and ****P* < 0.001 vs. siCTL (paired *t* test).

exons (Supplementary Fig. 3*C* and *D*). These results support the notion that SRp55, like most SR proteins (28), acts as a splicing activator, promoting exon inclusion when bound to exonic splicing enhancers. In line with this, the majority of modified cassette exons (73%) displayed exon skipping after SRp55 depletion (Supplementary Fig. 2*B*), suggesting that a large proportion of modified splicing events are directly regulated by SRp55. Motif enrichment also indicated that upregulated events were not directly regulated by SRp55 and probably result from the impact of SRp55 on other splicing regulators, as we previously observed after Nova1 KD (12).

Validation of Splicing Events

We next used independent EndoC-βH1 samples, different from the ones used for RNA sequencing, to confirm SRp55-regulated events. Representative genes of pathways regulating β-cell function and survival were selected for further

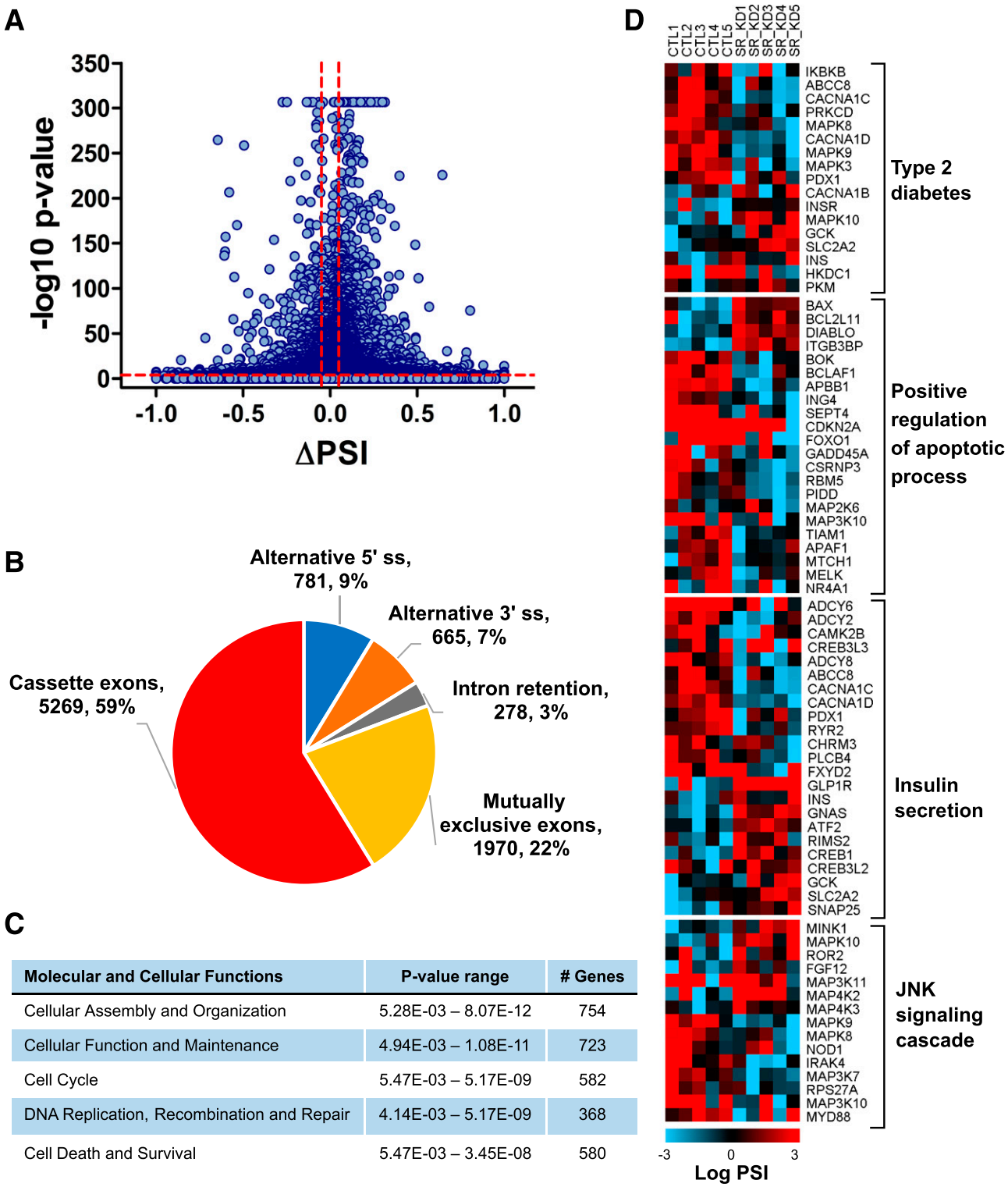

C

Molecular and Cellular Functions	P-value range	# Genes
Cellular Assembly and Organization	5.28E-03 – 8.07E-12	754
Cellular Function and Maintenance	4.94E-03 – 1.08E-11	723
Cell Cycle	5.47E-03 – 5.17E-09	582
DNA Replication, Recombination and Repair	4.14E-03 – 5.17E-09	368
Cell Death and Survival	5.47E-03 – 3.45E-08	580

Figure 2—RNA sequencing of EndoC-βH1 cells after SRp55 depletion. *A*: Pairwise comparison of control vs. SRp55 KD EndoC-βH1 cassette exons shown as a volcano plot. AS events presenting a difference of ΔPSI >5% and an FDR ≤0.01% were considered modified, as indicated by the dotted lines. *B*: Numbers and proportions of the different AS events modified after SRp55 silencing, as identified by rMATS analysis. *C*: Ingenuity pathway analysis of genes showing differential AS (enhanced or inhibited) after SRp55 depletion. *D*: Heat maps showing genes enriched with Gene Ontology terms involved in cell survival and β-cell function. PSI values are represented by gradient colors and shown for each individual control and SRp55 KD sample. Red represents a higher PSI; blue represents a lower PSI. Results are based on five RNA sequencing samples.

validation. We used RT-PCR followed by automated electrophoresis analysis based on primers that amplify isoforms presenting both inclusion and skipping of alternative fragments. We were able to validate 12 of 12 AS events tested (Fig. 3), indicating good reliability of the data generated by RNA sequencing.

SRp55 Silencing Impairs Insulin Release and Leads to Mitochondrial Dysfunction

SRp55-depleted cells showed impaired insulin secretion at 20 mmol/L glucose and in the presence of glucose plus forskolin, but their insulin content did not change (Fig. 4*A* and *B*). Insulin release is regulated by ATP generation, and

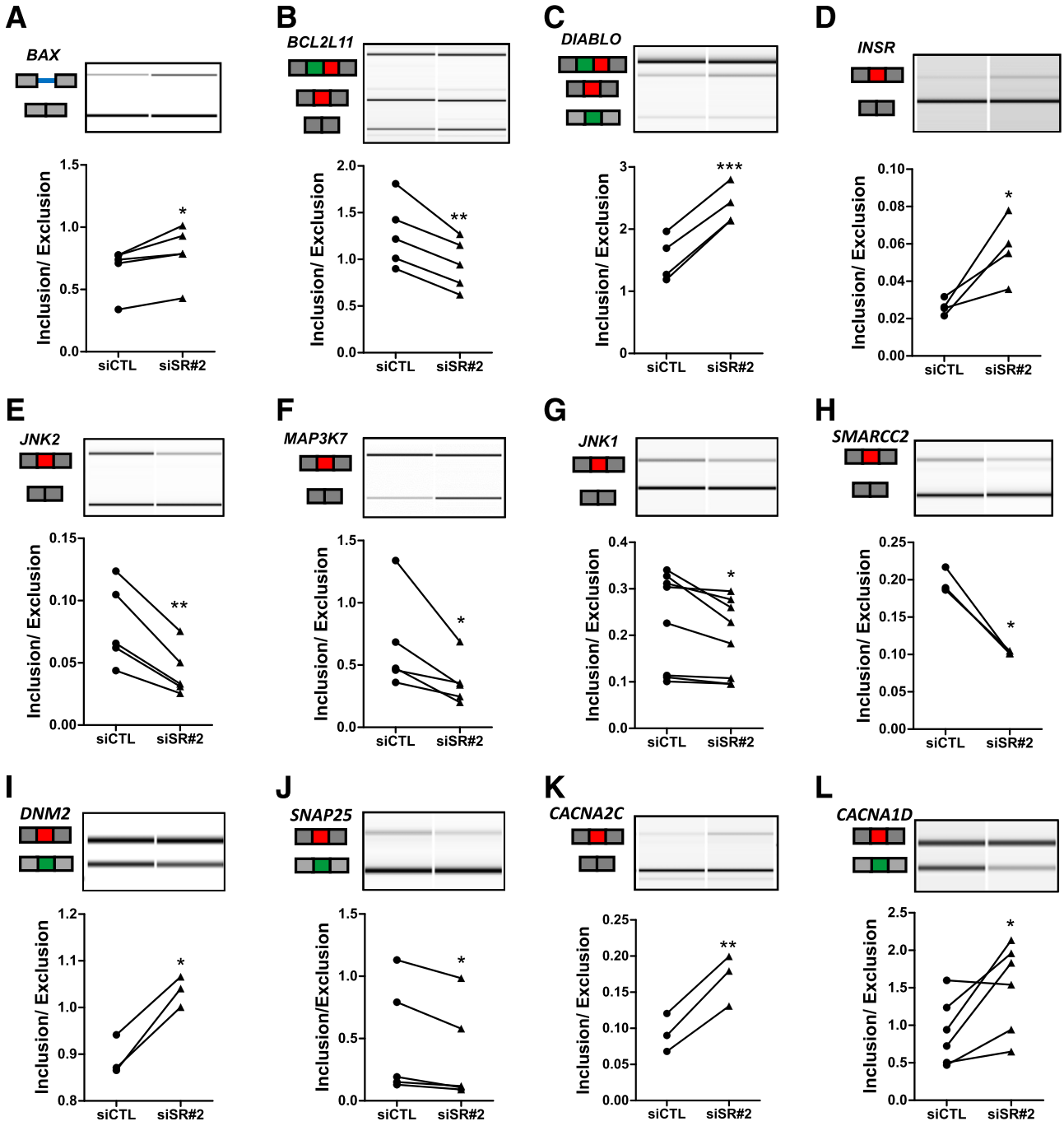

Figure 3—Confirmation of SRp55-regulated splicing events shown through representative RT-PCR validations (*A–L*). cDNA were amplified by RT-PCR using primers located in the upstream and downstream exons of the modified splicing event. PCR fragments were analyzed by automated electrophoresis using a bioanalyzer machine and quantified by comparison with a loading control. For each gene, representative gel images showing different splice variants affected by SRp55 KD and the corresponding inclusion-to-exclusion ratios are shown. The structure of each isoform is indicated by exons (blocks) and introns (solid lines). Alternatively spliced regions are indicated in red, green, or blue. Results are the mean ± SEM of three to eight independent experiments. *$P < 0.05$, **$P < 0.01$, and ***$P < 0.001$ vs. siCTL (paired *t* test).

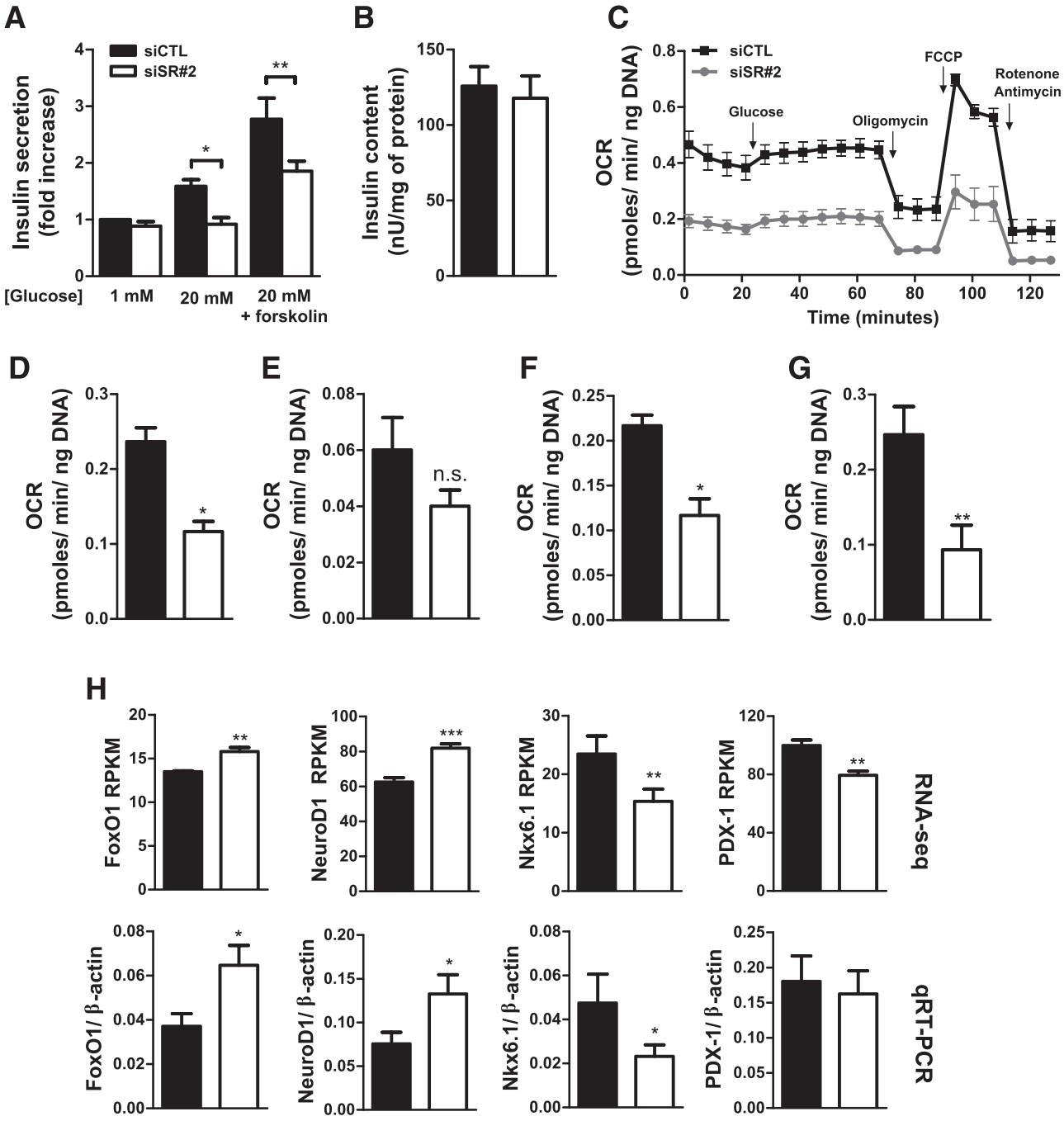

Figure 4—SRp55 depletion impairs insulin secretion and mitochondrial respiration. *A*: Insulin secretion in EndoC-βH1 cells was evaluated by ELISA after 1 h of stimulation with 1 mmol/L glucose, 20 mmol/L glucose, or 20 mmol/L glucose plus forskolin. *A*, *B*, and *D–H*: Black bars indicate transfection with control siRNA and white bars indicate transfection with siRNA against SRp55. *B*: Insulin content after SRp55 KD was evaluated by ELISA. *C–G*: Analysis of mitochondrial respiration parameters in EndoC-βH1 cells using a Seahorse oximeter. *C*: Oxygen consumption rate (OCR) profiles of control and SRp55 KD cells at basal conditions (1 mmol/L glucose) and after sequential treatment with glucose (20 mmol/L), oligomycin (5 μmol/L), FCCP (4 μmol/L), and rotenone plus antimycin A (1 μmol/L each). Injection of different compounds is indicated by arrows. *D*: Basal respiration (1 mmol/L glucose), calculated by subtracting nonmitochondrial respiration from the last measurement before 20 mmol/L glucose injection. *E*: Response to high glucose, calculated by subtracting the last basal respiration measurement from the last measurement after injection of 20 mmol/L glucose. *F*: ATP production, calculated by subtracting the minimum measurement after oligomycin injection from the last measurement after glucose injection. *G*: Maximal respiration, calculated by subtracting nonmitochondrial respiration from the maximum measurement after FCCP injection. *H*: mRNA expression of transcription factors regulating β-cell identity and phenotype. In the top panels, RNA sequencing expression values are shown in RPKM, and in the bottom panels, confirmation is indicated by quantitative RT-PCR (qRT-PCR) normalized by the housekeeping gene β-actin. Results are the mean ± SEM of three to nine experiments. $^{*}P < 0.05$, $^{**}P < 0.01$, and $^{***}P < 0.001$ vs. siCTL (ANOVA followed by the Bonferroni post hoc test [*A*] or the paired *t* test [*B* and *D–H*]).

we next analyzed mitochondrial respiration by assessing the oxygen consumption rate using a Seahorse metabolic analyzer. SRp55-depleted EndoC-βH1 cells showed decreased mitochondrial respiration when compared with control cells, exhibiting lower basal respiration, impaired ATP production (response to oligomycin), and decreased maximal respiration (response to FCCP after oligomycin) (Fig. 4*C–G*), suggesting that SRp55 silencing–induced mitochondrial dysfunction explains the observed defective glucose-induced insulin release.

Interestingly, RNA sequencing analysis indicated that several transcription factors that regulate the β-cell phenotype and affect insulin secretion were modified after SRp55 KD (Fig. 4*H*). This includes upregulation of *FOXO1* and *NEUROD1*, genes expressed in poorly differentiated endocrine cells (29), and downregulation of *PDX-1* and *NKX6.1*, key transcription factors for the maintenance of a differentiated β-cell phenotype (30,31).

SRp55 Contributes to β-Cell Apoptosis via Regulation of the Expression of Proapoptotic Splice Variants of BCL-2 Proteins

BCL-2 proteins are a family of apoptotic regulators that play a central role in β-cell survival (32). RNA sequencing analysis indicated that SRp55 regulates splicing of the BCL-2 proteins BIM (*BCL2L11*), BAX, and BOK, and of related apoptotic proteins DIABLO and BCLAF1 (Figs. 2 and 3). We previously showed that SRp55 KD in rat β-cells increases the expression of the most proapoptotic isoform Bim S (contributing to β-cell apoptosis) (9). Here we confirmed, at both the mRNA and protein levels, that SRp55 also regulates BIM splicing in human β-cells, increasing the proportion of BIM S over BIM L after SRp55 depletion (Fig. 3*B* and Supplementary Fig. 4*A* and *B*). An overall increase of BIM isoforms also occurred after SRp55 silencing (Supplementary Fig. 4*A* and *C*). To assess the functional role of BIM in SRp55 KD–induced apoptosis, we performed a double KD of SRp55 and BIM (Supplementary Fig. 4*D–F*). BIM inhibition decreased EndoC-βH1 apoptosis to basal levels (Supplementary Fig. 4*F*), indicating that BIM plays a central role in regulating cell death in SRp55-depleted cells and suggesting that SRp55 depletion triggers the intrinsic or mitochondrial pathway of apoptosis.

SRp55 depletion also affected splicing of the apoptotic effector protein BAX, leading to increased intron 5 retention (Figs. 3*A* and 5*A*). Unspliced intron 5 leads to the production of BAX β, a constitutively active isoform that may trigger cell death independent of upstream signaling (33) (Fig. 5*B*). To test whether alteration of BAX splicing by SRp55 KD contributes to the observed increase in apoptosis, we designed a specific BAX β siRNA and performed single and double KD experiments in combination with SRp55 siRNA (Figs. 5*C–F*). The upregulation of BAX β after SRp55 KD (Fig. 5*E*) correlated with increased BAX translocation to the mitochondria (Fig. 5*C*) and increased apoptosis (Fig. 5*F*). Prevention of a BAX β increase by a specific siRNA in SRp55-depleted cells (Fig. 5*E*) reduced BAX translocation to the mitochondria (Fig. 5*C*) and protected EndoC-βH1 cells (Fig. 5*F*) and human islets (Fig. 5*G*) against apoptosis, indicating a contributory role for BAX β in the observed phenotype.

SRp55 Depletion Affects the JNK Signaling Pathway, Leading to Pathway Hyperactivation and Increased β-Cell Apoptosis

The JNK pathway has a proapoptotic role in pancreatic β-cells (34,35). RNA sequencing analysis indicated that SRp55 KD affects the splicing of several members of the JNK pathway (Figs. 2*D*, 3*E–G*, and 6*A*). Moreover, several JNK signaling genes are upregulated after SRp55 silencing (Supplementary Table 6). To understand how these alterations affect JNK pathway activity, we first analyzed the phosphorylation state of the kinases MKK7 and JNK1, and the target transcription factor c-JUN. We observed that MKK7, JNK1, and c-JUN are hyperphosphorylated in SRp55-depeleted cells, whereas no changes in total protein levels were observed for MKK7 and JNK1 (Fig. 6*B*). We hypothesized that splicing alterations in JNK-related signaling genes alter the pathway activity, contributing to increased β-cell death. To test this, we first performed a double KD of JNK1 and SRp55. Inhibition of JNK1 in both EndoC-βH1 cells and human islets protected them against SRp55 KD–induced apoptosis (Fig. 6*C–F*). Next, we mimicked the impact of SRp55 depletion on the splicing of three JNK signaling kinases (*MAP3K7*, *JNK1*, and *JNK2*) using specific siRNAs against the SRp55-modified cassette exons in these genes. These siRNAs significantly increased the skipping of the cassette exons, recapitulating the effect of SRp55 KD (Figs. 6*G–I*). It is interesting to note that increased exon skipping in all three JNK-related genes was associated with increased apoptosis (Fig. 6*J*) and JNK hyperphosphorylation (Fig. 6*K*) in EndoC-βH1 cells. This supports the hypothesis that splicing alterations induced by SRp55 KD lead to hyperactivation of the JNK-regulated pathway and contribute to β-cell death.

SRp55 Depletion Induces Endoplasmic Reticulum Stress

RNA sequencing analysis showed that several genes of the endoplasmic reticulum (ER)–associated protein degradation pathway displayed AS alterations after SRp55 depletion and that some ER stress markers were upregulated at the gene expression level (Fig. 7*A*). These findings suggest that reduced SRp55 levels affect ER function and may contribute to increased β-cell apoptosis. To test this hypothesis, we analyzed the expression of several ER stress markers at the protein and mRNA levels. Increased levels of phosphorylated and total IRE1α (Fig. 7*B* and *C*) and phospho-eIF2α (Fig. 7*B* and *E*) were observed after SRp55 silencing. Moreover, induction of *BIP* (Fig. 7*F*) and *XBP1* (Fig. 7*G*) spliced mRNA was detected by quantitative PCR, indicating that SRp55 deficiency may directly or indirectly lead to ER stress. No significant changes, however, were observed for phosphorylated and total *PERK* and *CHOP* (Fig. 7*D* and *H*). To determine whether ER stress indeed contributes to SRp55 KD–induced apoptosis, we performed double KD of IRE1α and SRp55 (Fig. 7*I* and *J*). IRE1α silencing protected EndoC-βH1 cells against death induced by SRp55

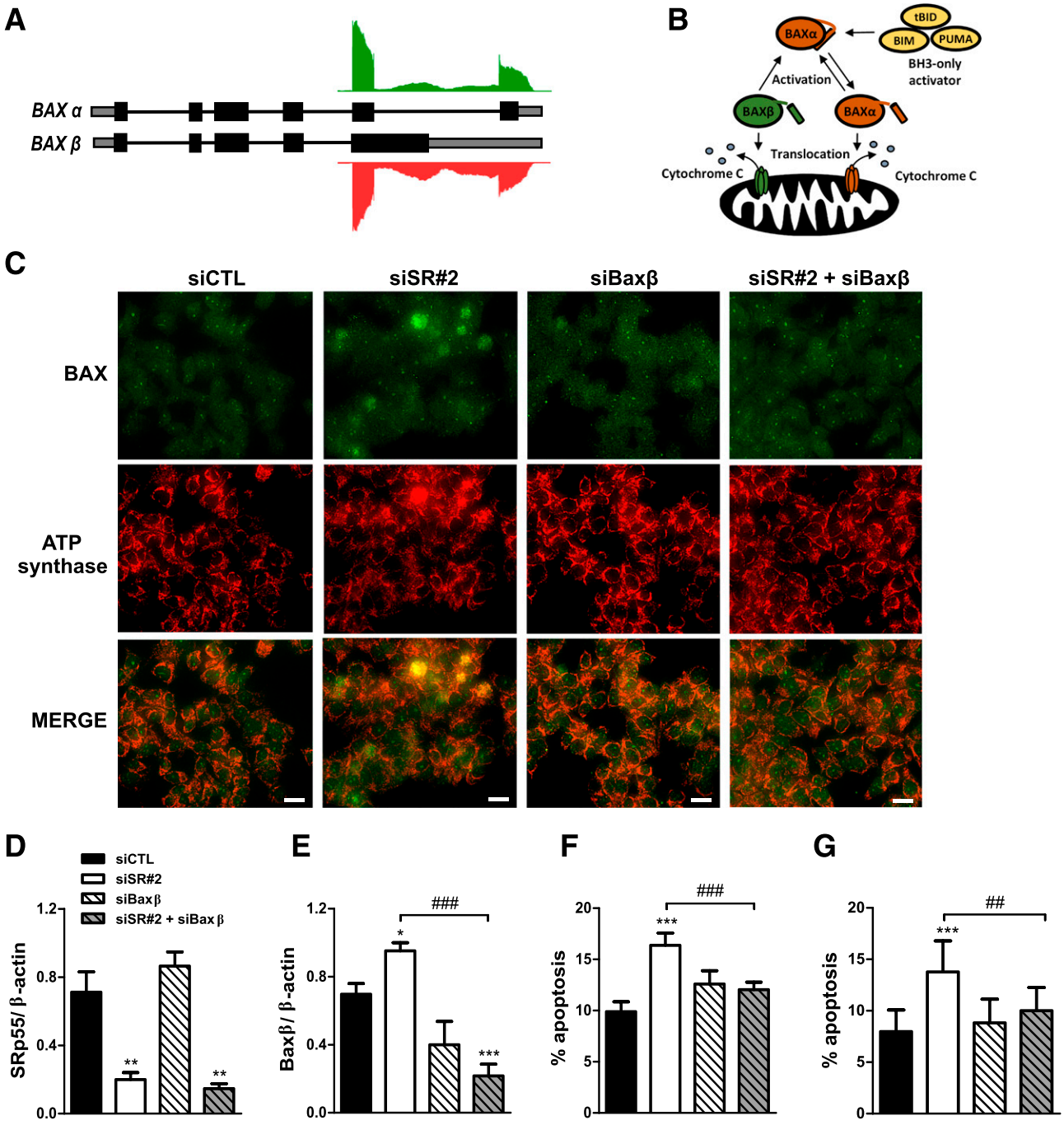

Figure 5—SRp55 controls the expression of a constitutively active isoform of the apoptotic inducer BAX, contributing to increased β-cell apoptosis. *A*: Schematic representation of *BAX* isoforms α and β, and RNA sequencing reads in control and SRp55 KD cells mapping to the distal part of the gene. Boxes represent exons; gray represents untranslated regions; black represents coding regions; and solid lines represent introns. *B*: Model of activation of apoptosis by BAX α and BAX β isoforms proposed by Fu et al. (33). Upon apoptotic signaling, BH3-only molecules such as BIM activate BAX α to promote its translocation and oligomerization to the mitochondrial outer membrane, leading to cytochrome c release and apoptosis activation. On the other hand, BAX β spontaneously targets, oligomerizes, and permeabilizes mitochondria, behaving as a constitutively active isoform. *C–G*: Double KD of SRp55 and BAX β in EndoC-βH1 cells (*C–F*) and in human islets (*G*). Cells were transfected with siCTL, siSR#2, siBaxβ, or siSR#2 plus siBaxβ for 48 h. *C*: Fluorescence microscopy analysis of BAX and the mitochondrial marker ATP synthase in EndoC-βH1 cells, showing that SRp55 KD leads to increased translocation of BAX to the mitochondria, a phenomenon prevented by BAX β silencing. Scale bar = 1 μm. mRNA expression of SRp55 (*D*) and BAX β (*E*) was measured by quantitative RT-PCR and normalized by the housekeeping gene β-actin. mRNA expression values were normalized by the highest value of each experiment, considered as 1. Proportion of apoptotic cells in EndoC-βH1 cells (*F*) and in dispersed human islets (*G*). Results are the mean ± SEM of four or five independent experiments. $^{*}P < 0.05$, $^{**}P < 0.01$, and $^{***}P < 0.001$ vs. siCTL; $\#\#P < 0.01$ and $\#\#\#P < 0.001$ as indicated by bars (ANOVA followed by the Bonferroni post hoc test).

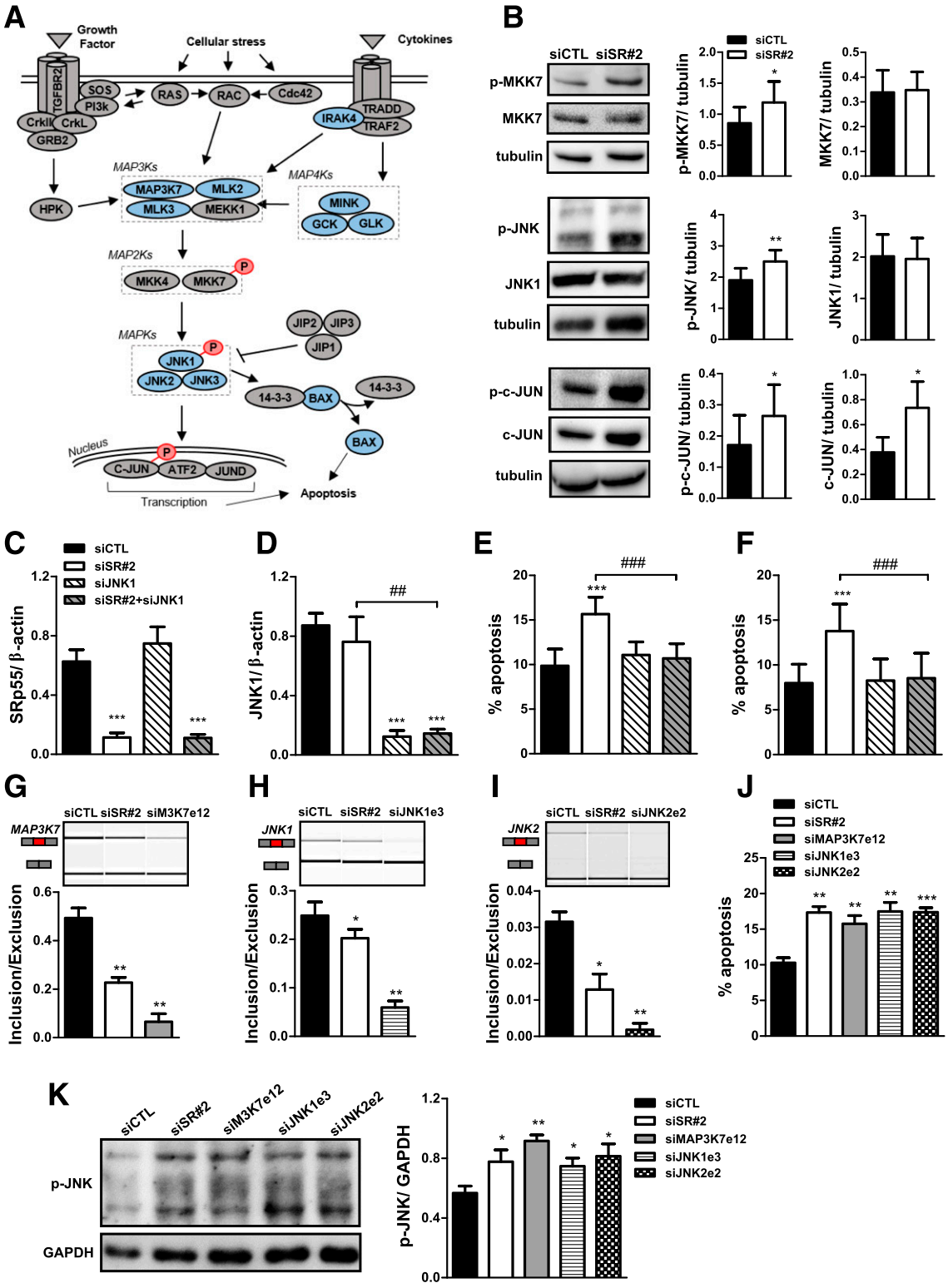

Figure 6—SRp55 modifies the splicing of JNK signaling cascade genes, leading to JNK1 hyperactivation and β-cell apoptosis. *A*: Schematic representation of the JNK signaling pathway. Proteins showing AS detected by RNA sequencing after SRp55 KD are shown in blue. Proteins exhibiting overphosphorylation upon SRp55 depletion are shown in red. *B*: Representative Western blotting and densitometric measurements of total and phosphorylated forms of MKK7, JNK1, and c-JUN in EndoC-βH1 cells under control conditions and after SRp55 KD. *C–F*: Double KD of SRp55 and JNK1 in EndoC-βH1 cells (*C–E*) and in human islets (*F*). Cells were transfected with siCTL, siSR#2, siJNK1, or siSR#2 plus siJNK1 for 48 h. mRNA expression of SRp55 (*C*) and JNK1 (*D*) was measured by quantitative RT-PCR and normalized by the housekeeping gene β-actin. mRNA expression values were normalized by the highest value of each experiment, considered as 1. *E* and *F*: Proportion of apoptotic cells in EndoC-βH1 cells (*E*) and in dispersed human islets (*F*). *G–K*: Specific KD of three SRp55-regulated spliced variants of the JNK cascade. EndoC-βH1 cells were transfected with siCTL, siSR#2, or specific siRNA targeting cassette exons of MAP3K7 (exon 12, siMAP3K7e12), JNK1

deficiency (Fig. 7*K*), demonstrating that defects in ER homeostasis and consequent ER stress promote apoptosis in SRp55-depleted cells.

DISCUSSION

These findings indicate that SRp55 drives a crucial splicing program to preserve human pancreatic β-cell survival and function. SRp55 is highly expressed in human pancreatic β-cells, and its depletion leads to β-cell apoptosis and impaired insulin secretion. SRp55 levels are downregulated by proinflammatory cytokines and may contribute to cytokine-induced β-cell apoptosis. These observations suggest that SRp55 acts as a master splicing regulator of β-cell survival under both basal and immune-induced stress conditions. In line with these observations, SRp55 regulates AS of multiple transcripts involved in cell death, JNK signaling, insulin secretion, and ER stress, providing a mechanistic link between the observed phenotype and SRp55 targets.

Our group previously showed that SRp55 is transcriptionally regulated by the transcription factor *Glis3* (9). The *GLIS3* locus is associated with T1D and T2D (4,5) and with glucose metabolism traits in subjects without diabetes (36), and its inactivation leads to a severe form of monogenic diabetes in humans (6,37). *GLIS3* is also required for β-cell survival (9), and defective *Glis3* expression affects the unfolded protein response promoting β-cell fragility (38). We observed in these experiments that decreased SRp55 expression recapitulates many of the pathological features induced by *GLIS3* deficiency, for example, increased β-cell apoptosis, defective insulin release, and ER stress, suggesting that SRp55 may act as an important downstream mediator of *GLIS3* function.

AS modulates the function of many BCL-2 proteins and other apoptotic regulators, producing variants that differ in their localization, posttranslation regulation, or proapoptotic activity (39,40). Our RNA sequencing analysis revealed that SRp55 regulates several genes involved in pancreatic β-cell apoptosis, including several BCL-2 proteins. It is important to note that SRp55 depletion affects the splicing of the apoptotic activator BAX, promoting the expression of the constitutively active isoform BAX β. The canonical isoform BAX α contains a COOH-terminal transmembrane domain tucked into the dimerization pocket that maintains BAX α in an autoinhibited monomeric conformation in the cytosol. After proapoptotic signaling, BH3-only activators such as BIM and PUMA induce a conformational change on BAX α, promoting its oligomerization, its translocation to the mitochondria, permeabilization of the outer membrane, and activation of apoptosis (41). BAX β, on the other hand, retains intron 5, creating a distinct COOH-terminal domain that maintains it in a permanently activated conformation, leading to its spontaneous oligomerization and activation of apoptosis (33). In addition, BAX β can also act as a BH3-only activator able to activate BAX α (33). BAX α may also be activated by BIM S (42), shown here to be induced by SRp55 KD. The fact that independent KD of BAX β or BIM nearly completely prevents the increase in β-cell apoptosis observed after SRp55 KD suggests that both mechanisms are required to trigger the intrinsic pathway of apoptosis under these experimental conditions.

It is interesting that our data indicate that SRp55 regulates two other pathways potentially involved in β-cell death in cross talk with BCL-2 proteins, namely the JNK signaling cascade and ER stress. The JNK pathway has a pivotal role in integrating different stress signals and in promoting β-cell death (32,43,44). JNK1 signaling stimulates the transcription and activity of proapoptotic BCL-2 proteins through activation of the transcription factor c-JUN and through direct phosphorylation (32). Moreover, the JNK pathway is also activated by ER stress via the transmembrane protein IRE1α (45). Different JNK splice variants may differ in their enzymatic activities, substrates, and activation/deactivation kinetics (46,47). For instance, a single splice change in MKK7 is able to increase the JNK pathway activity in T cells (48). SRp55 depletion affects the splicing of several kinases of the JNK signaling cascade (as shown by the data presented here). These findings indicate that some of these changes modify the basal activity of the pathway, leading to JNK hyperactivation and contributing to β-cell apoptosis. JNK hyperactivation may also be secondary to the unfolded protein response via IRE1α signaling (45). We observed that SRp55 silencing induces basal ER stress. The mechanisms by which SRp55 deficiency triggers ER stress remains to be clarified, but splicing alterations in ER-associated protein degradation genes suggest that ER function may be compromised through defective disposal of terminally misfolded proteins.

Reduced SRp55 expression also leads to impaired insulin release. Insulin exocytosis is tightly coupled to glucose metabolism, requiring mitochondrial ATP production to induce the closure of K_{ATP} channels and the generation of Ca^{2+} influx that ultimately triggers the release of insulin (49). Our findings suggest that impaired insulin release induced by glucose is related to mitochondrial dysfunction. Furthermore, SRp55 silencing modifies the expression of genes and splice variants related to metabolic pathways, exocytosis, and calcium signaling, all of which potentially affect the regulation of insulin secretion. The findings

(exon 3, siJNK1e3), and JNK2 (exon 2, siJNK2e2). *G–I*: Representative RT-PCR validations showing increased exon skipping in *MAP3K7* (*G*), *JNK1* (*H*), and *JNK2* (*I*). *J* and *K*: Percentage of apoptotic cells (*J*) and JNK phosphorylation (*K*) after SRp55 KD or skipping of *MAP3K7*, *JNK1*, and *JNK2* cassette exons. Results are the mean ± SEM of four or five independent experiments. $^{*}P < 0.05$, $^{**}P < 0.01$, and $^{***}P < 0.001$ vs. siCTL; $\#\#P < 0.01$ and $\#\#\#P < 0.001$ as indicated by bars (paired *t* test [*B*, *G–K*] or ANOVA followed by the Bonferroni post hoc test [*C–F*]).

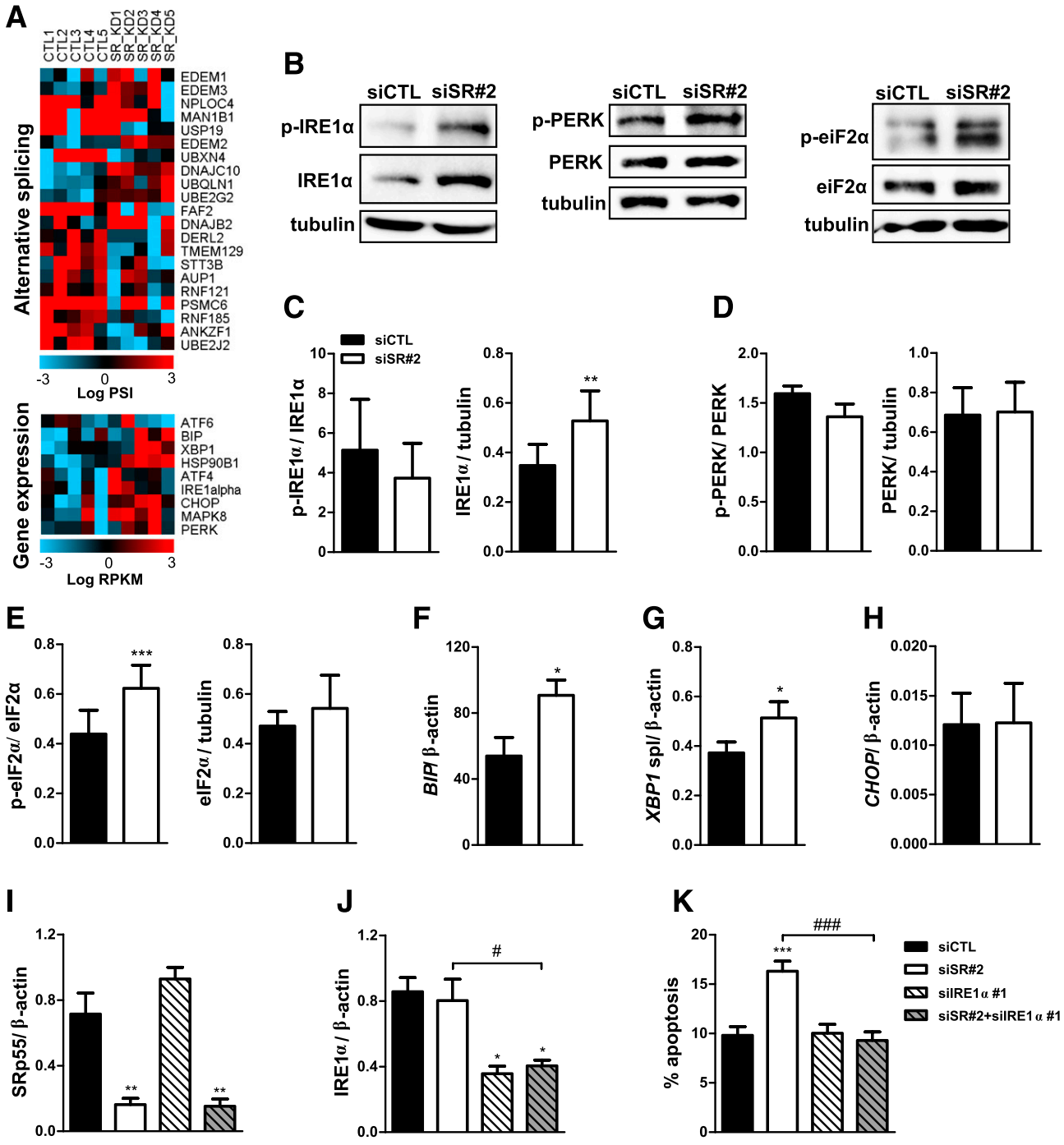

Figure 7—SRp55 KD–induced ER stress contributes to β-cell death. *A*: Heat map showing AS and gene expression changes in genes involved in the ER-associated protein degradation process (top panel) and markers of the unfolded protein response (bottom panel). Red represents higher expression and blue, lower expression. *B–E*: Representative Western blotting (*B*) and densitometric measurements of total and phosphorylated forms of IRE1α (*C*), PERK (*D*), and eIF2α (*E*). mRNA expression of *BIP* (*F*), *XBP1* spliced (*G*), and *CHOP* (*H*) after SRp55 KD was measured by quantitative RT-PCR (qRT-PCR) and normalized by the housekeeping gene β-actin. *I–K*: Double KD of SRp55 and IRE1α in EndoC-βH1 cells. Cells were transfected with siCTL, siSR#2, siIRE1α, or siSR#2 plus siIRE1α for 48 h. mRNA expression of SRp55 (*I*) and IRE1α (*J*) was measured by qRT-PCR and normalized by the housekeeping gene β-actin. mRNA expression values were normalized by the highest value of each experiment, considered as 1. *K*: The proportion of apoptotic cells was evaluated by Hoechst/propidium iodide staining. Results are the mean ± SEM of four to nine independent experiments. $^{*}P < 0.05$, $^{**}P < 0.01$, and $^{***}P < 0.001$ vs. siCTL; $\#P < 0.05$ and $\#\#\#P < 0.001$ as indicated by bars (paired *t* test [*C–H*] or ANOVA followed by the Bonferroni post hoc test [*I–K*]).

described here are, however, correlative, and the precise mechanisms by which SRp55 depletion impairs β-cell function remain to be clarified.

In conclusion, the observations presented here indicate that SRp55 coordinates a splicing network of functionally interconnected genes in β-cells. These genes are required

for β-cell survival and a functional phenotype. This suggests that alterations in SRp55—for instance, downstream of polymorphisms that decrease activity of the diabetes candidate gene *GLIS3*—may promote β-cell failure and loss in diabetes.

Acknowledgments. The authors are grateful to Isabelle Millard, Anyishaï Musuaya, Nathalie Pachera, and Michaël Pangerl of the ULB Center for Diabetes Research for providing excellent technical support. The authors thank Hirokazu Hara (Gifu Pharmaceutical University, Gifu, Japan) for providing the human SRp55 expression plasmid.

Funding. This work was supported by grants from the Fonds National de la Recherche Scientifique Belgique (FNRS) (WELBIO CR-2015A-06), the Horizon 2020 Framework Programme (T2DSYSTEMS, GA667191), and the National Institutes of Health, National Institute of Diabetes and Digestive Kidney Diseases, and Human Islet Research Network Consortium (1UC4DK104166-01). J.J.-M. was supported by an H2020 Marie Skłodowska-Curie Actions fellowship grant (project reference 660449). M.I.A. was supported by a FRIA fellowship from the FNRS (reference no. 26410496). P.M. and D.L.E. have received funding from the Innovative Medicines Initiative 2 Joint Undertaking under grant agreement no. 115797 (INNODIA). This Joint Undertaking receives support from the European Union's Horizon 2020 research and innovation programme and the European Federation of Pharmaceutical Industries and Associations, the JDRF, and the Leona M. and Harry B. Helmsley Charitable Trust.

Duality of Interest. No conflicts of interest relevant to this article were reported.

Author Contributions. J.J.-M., M.I.A., and D.L.E. conceived and designed the experiments and wrote the manuscript. J.J.-M., M.I.A., J.-V.T., O.V., E.L.-M., F.A.G., and L.M. acquired data. M.B. and P.M. contributed material and reagents. All authors revised the manuscript. J.J.-M. and D.L.E. are the guarantors of this work and, as such, had full access to all the data in the study and take responsibility for the integrity of the data and the accuracy of the data analysis.

References

1. Cnop M, Welsh N, Jonas JC, Jörns A, Lenzen S, Eizirik DL. Mechanisms of pancreatic beta-cell death in type 1 and type 2 diabetes: many differences, few similarities. Diabetes 2005;54(Suppl. 2):S97–S107

2. Rahier J, Guiot Y, Goebbels RM, Sempoux C, Henquin JC. Pancreatic beta-cell mass in European subjects with type 2 diabetes. Diabetes Obes Metab 2008; 10(Suppl. 4):32–42

3. Campbell-Thompson M, Fu A, Kaddis JS, et al. Insulitis and β-cell mass in the natural history of type 1 diabetes. Diabetes 2016;65:719–731

4. Barrett JC, Clayton DG, Concannon P, et al.; Type 1 Diabetes Genetics Consortium. Genome-wide association study and meta-analysis find that over 40 loci affect risk of type 1 diabetes. Nat Genet 2009;41:703–707

5. Dupuis J, Langenberg C, Prokopenko I, et al.; DIAGRAM Consortium; GIANT Consortium; Global BPgen Consortium; Anders Hamsten on behalf of Procardis Consortium; MAGIC investigators. New genetic loci implicated in fasting glucose homeostasis and their impact on type 2 diabetes risk. Nat Genet 2010;42:105–116

6. Senée V, Chelala C, Duchatelet S, et al. Mutations in GLIS3 are responsible for a rare syndrome with neonatal diabetes mellitus and congenital hypothyroidism. Nat Genet 2006;38:682–687

7. ZeRuth GT, Takeda Y, Jetten AM. The Krüppel-like protein Gli-similar 3 (Glis3) functions as a key regulator of insulin transcription. Mol Endocrinol 2013;27:1692–1705

8. Yang Y, Chang BH, Yechoor V, et al. The Krüppel-like zinc finger protein GLIS3 transactivates neurogenin 3 for proper fetal pancreatic islet differentiation in mice. Diabetologia 2011;54:2595–2605

9. Nogueira TC, Paula FM, Villate O, et al. GLIS3, a susceptibility gene for type 1 and type 2 diabetes, modulates pancreatic beta cell apoptosis via regulation of a splice variant of the BH3-only protein Bim. PLoS Genet 2013;9:e1003532

10. Calarco JA, Zhen M, Blencowe BJ. Networking in a global world: establishing functional connections between neural splicing regulators and their target transcripts. RNA 2011;17:775–791

11. Papasaikas P, Rao A, Huggins P, Valcarcel J, Lopez A. Reconstruction of composite regulator-target splicing networks from high-throughput transcriptome data. BMC Genomics 2015;16(Suppl. 10):S7

12. Villate O, Turatsinze JV, Mascali LG, et al. Nova1 is a master regulator of alternative splicing in pancreatic beta cells. Nucleic Acids Res 2014;42:11818–11830

13. Juan-Mateu J, Rech TH, Villate O, et al. Neuron-enriched RNA-binding proteins regulate pancreatic beta cell function and survival. J Biol Chem 2017;292: 3466–3480

14. Eizirik DL, Sammeth M, Bouckenooghe T, et al. The human pancreatic islet transcriptome: expression of candidate genes for type 1 diabetes and the impact of pro-inflammatory cytokines. PLoS Genet 2012;8:e1002552

15. Juan-Mateu J, Villate O, Eizirik DL. Mechanisms in endocrinology: alternative splicing: the new frontier in diabetes research. Eur J Endocrinol 2016;174:R225–R238

16. Cohen-Eliav M, Golan-Gerstl R, Siegfried Z, et al. The splicing factor SRSF6 is amplified and is an oncoprotein in lung and colon cancers. J Pathol 2013;229:630–639

17. Jensen MA, Wilkinson JE, Krainer AR. Splicing factor SRSF6 promotes hyperplasia of sensitized skin. Nat Struct Mol Biol 2014;21:189–197

18. Ravassard P, Hazhouz Y, Pechberty S, et al. A genetically engineered human pancreatic beta cell line exhibiting glucose-inducible insulin secretion. J Clin Invest 2011;121:3589–3597

19. Kutlu B, Cardozo AK, Darville MI, et al. Discovery of gene networks regulating cytokine-induced dysfunction and apoptosis in insulin-producing INS-1 cells. Diabetes 2003;52:2701–2719

20. Eizirik DL, Sammeth M, Bouckenooghe T, et al. The human pancreatic islet transcriptome: expression of candidate genes for type 1 diabetes and the impact of pro-inflammatory cytokines. PLoS Genet 2012;8:e1002552

21. Montgomery SB, Sammeth M, Gutierrez-Arcelus M, et al. Transcriptome genetics using second generation sequencing in a Caucasian population. Nature 2010;464:773–777

22. Shen S, Park JW, Lu ZX, et al. rMATS: robust and flexible detection of differential alternative splicing from replicate RNA-Seq data. Proc Natl Acad Sci U S A 2014;111:E5593–E5601

23. Park JW, Jung S, Rouchka EC, Tseng YT, Xing Y. rMAPS: RNA map analysis and plotting server for alternative exon regulation. Nucleic Acids Res 2016;44(W1): W333–W338

24. Liu HX, Zhang M, Krainer AR. Identification of functional exonic splicing enhancer motifs recognized by individual SR proteins. Genes Dev 1998;12: 1998–2012

25. Huang da W, Sherman BT, Lempicki RA. Bioinformatics enrichment tools: paths toward the comprehensive functional analysis of large gene lists. Nucleic Acids Res 2009;37:1–13

26. Overbergh L, Valckx D, Waer M, Mathieu C. Quantification of murine cytokine mRNAs using real time quantitative reverse transcriptase PCR. Cytokine 1999; 11:305–312

27. Andersson LE, Valtat B, Bagge A, et al. Characterization of stimulus-secretion coupling in the human pancreatic EndoC-βH1 beta cell line. PLoS One 2015;10: e0120879

28. Jeong S. SR proteins: Binders, regulators, and connectors of RNA. Mol Cells 2017;40:1–9

29. Jiang Z, Tian J, Zhang W, et al. Forkhead protein FoxO1 acts as a repressor to inhibit cell differentiation in human fetal pancreatic progenitor cells. J Diabetes Res 2017;2017:6726901

30. Schaffer AE, Taylor BL, Benthuysen JR, et al. Nkx6.1 controls a gene regulatory network required for establishing and maintaining pancreatic Beta cell identity. PLoS Genet 2013;9:e1003274

31. Dassaye R, Naidoo S, Cerf ME. Transcription factor regulation of pancreatic organogenesis, differentiation and maturation. Islets 2016;8:13–34

32. Gurzov EN, Eizirik DL. Bcl-2 proteins in diabetes: mitochondrial pathways of β-cell death and dysfunction. Trends Cell Biol 2011;21:424–431
33. Fu NY, Sukumaran SK, Kerk SY, Yu VC. Baxbeta: a constitutively active human Bax isoform that is under tight regulatory control by the proteasomal degradation mechanism. Mol Cell 2009;33:15–29
34. Mokhtari D, Myers JW, Welsh N. The MAPK kinase kinase-1 is essential for stress-induced pancreatic islet cell death. Endocrinology 2008;149:3046–3053
35. Gurzov EN, Ortis F, Bakiri L, Wagner EF, Eizirik DL. JunB inhibits ER stress and apoptosis in pancreatic beta cells. PLoS One 2008;3:e3030
36. Boesgaard TW, Grarup N, Jørgensen T, Borch-Johnsen K, Hansen T, Pedersen O; Meta-Analysis of Glucose and Insulin-Related Trait Consortium (MAGIC). Variants at DGKB/TMEM195, ADRA2A, GLIS3 and C2CD4B loci are associated with reduced glucose-stimulated beta cell function in middle-aged Danish people. Diabetologia 2010;53:1647–1655
37. Dimitri P, Habeb AM, Gurbuz F, et al. Expanding the clinical spectrum associated with GLIS3 mutations[published correction appears in J Clin Endocrinol Metab 2015;100:4685]. J Clin Endocrinol Metab 2015;100:E1362–E1369
38. Dooley J, Tian L, Schonefeldt S, et al. Genetic predisposition for beta cell fragility underlies type 1 and type 2 diabetes. Nat Genet 2016;48:519–527
39. Akgul C, Moulding DA, Edwards SW. Alternative splicing of Bcl-2-related genes: functional consequences and potential therapeutic applications. Cell Mol Life Sci 2004;61:2189–2199
40. Schwerk C, Schulze-Osthoff K. Regulation of apoptosis by alternative pre-mRNA splicing. Mol Cell 2005;19:1–13
41. Annis MG, Soucie EL, Dlugosz PJ, et al. Bax forms multispanning monomers that oligomerize to permeabilize membranes during apoptosis. EMBO J 2005;24:2096–2103
42. Marani M, Tenev T, Hancock D, Downward J, Lemoine NR. Identification of novel isoforms of the BH3 domain protein Bim which directly activate Bax to trigger apoptosis. Mol Cell Biol 2002;22:3577–3589
43. Cunha DA, Hekerman P, Ladrière L, et al. Initiation and execution of lipotoxic ER stress in pancreatic beta-cells. J Cell Sci 2008;121:2308–2318
44. Cunha DA, Igoillo-Esteve M, Gurzov EN, et al. Death protein 5 and p53-upregulated modulator of apoptosis mediate the endoplasmic reticulum stress-mitochondrial dialog triggering lipotoxic rodent and human β-cell apoptosis. Diabetes 2012;61:2763–2775
45. Urano F, Wang X, Bertolotti A, et al. Coupling of stress in the ER to activation of JNK protein kinases by transmembrane protein kinase IRE1. Science 2000;287:664–666
46. Figuera-Losada M, LoGrasso PV. Enzyme kinetics and interaction studies for human JNK1β1 and substrates activating transcription factor 2 (ATF2) and c-Jun N-terminal kinase (c-Jun). J Biol Chem 2012;287:13291–13302
47. Zeke A, Misheva M, Reményi A, Bogoyevitch MA. JNK signaling: regulation and functions based on complex protein-protein partnerships. Microbiol Mol Biol Rev 2016;80:793–835
48. Martinez NM, Agosto L, Qiu J, et al. Widespread JNK-dependent alternative splicing induces a positive feedback loop through CELF2-mediated regulation of MKK7 during T-cell activation. Genes Dev 2015;29:2054–2066
49. Henquin JC. The dual control of insulin secretion by glucose involves triggering and amplifying pathways in β-cells. Diabetes Res Clin Pract 2011;93(Suppl. 1): S27–S31